

Effects of underground circular void on strip footing laid on the edge of a cohesionless slope under eccentric loads

Tarek Mansouri¹ , Rafik Boufarh^{2#} , Djamel Saadi² 

Article

Keywords

Strip footing
Eccentric load
Slope
Underground void
Sand
Bearing capacity

Abstract

Owing to the comeback of small-scale models, this paper presents results of an experimental study based on the effect of underground circular voids on strip footing placed on the edge of a cohesionless slope and subjected to eccentric loads. The bearing capacity-settlement relationship of footing on the slope and impact of diverse variables are expressed using dimensionless parameters such as the top vertical distance of the void from the base of footing, horizontal space linking the void-footing centre, and load eccentricity. The results verified that the stability of strip footing is influenced by the underground void, as well as the critical depth between the soil and top layer of the void. The critical horizontal distance between the void and the centre was also affected by the underground void. Furthermore, the results also verified that the influence of the void appeared insignificant when it was positioned at a depth or eccentricity equal to twice the width of footing.

1. Introduction

The existence of an underground void on a foundation can cause serious engineering problems that destabilize it and expose its superstructure to severe damage, which could be very expensive and hazardous. The presence of underground voids negatively affects the ultimate bearing capacity of superficial foundations. Underground cavities that cross the subsoil can be generally categorized into two: artificial and natural. Artificial or man-made cavities result from urban installation, tunnelling, mining, and old conduits, including water and gas networks. Natural cavities are shaped by the dissolution of sedimentary rocks owing to the circulation of water (karst and natural gypsum), which forms cavities of widely varying sizes. In engineering practice, the existence of voids in the ground compromises the bearing capacity and structural integrity of foundations. These cavities indicate a very significant potential risk of collapse, especially in urban sectors where the stakes are high. Frequently, footings are positioned on a soil with voids that are either hidden before building or shaped after it. Extensive analytical and model studies have been carried out to investigate the behaviour of such soil. Several researchers have dealt with the impact of voids on the ultimate bearing capacity of foundations. Researchers such as (Atkinson & Potts, 1977; Badie & Wang, 1984; Baus & Wang, 1983; Wang & Badie, 1985) pioneered studies on voids and the load-carrying capacity of footing stability. They demonstrated how the presence of voids affects a certain critical region under the footing.

The size of the critical region depends on numerous factors, such as: footing shape, soil property, void size, and void shape. Wang & Hsieh (1987) investigated the collapsed load of strip foundation on circular voids via the limit analysis theory, in which he reviewed several failure mechanisms. In 'Natural and artificial cavities as ground engineering hazards', Culshaw & Waltham (1987) briefly presented the different types of cavities, outlining the mode of creation and history of natural and artificial cavities, respectively. They proposed an outline process for tracing cavities and decreasing the risk of omission during site explorations. Then, via numerical analysis, Kiyosumi et al. (2007) determined that the failure zone emerged mainly from the adjacent footing-void and did not usually expand to other cavities. Additionally, this failure was less significant in soils without voids. A computational method was developed to approximately determine the yielding pressure of strip footing over numerous holes. Addressing the impact of voids on foundation stability, another research by Khalil & Khattab (2009) adopted a non-linear finite elements analysis method. The study verified that a significant zone exists under the footing 'radial shear and failure plane zone'. If a void is placed inside this zone, then the result will be critical. Settlement rate was observed for voids positioned in this zone below the foundation.

The experimental observation of Kiyosumi et al. (2011) demonstrated three sorts of failure modes for a single void, according to the void's size and position. Upper-bound calculations were presented to interpret the observed changes in bearing capacity. Mohamed (2012) carried out a numerical

#Corresponding author. E-mail address: rafik.boufarh@univ-tebessa.dz

¹University of Batna 2, Faculty of Technology, Department of Civil Engineering, Research Laboratory in Hydraulic Applied LARHA, Batna, Algeria.

²Larbi Tebessi University, Faculty of Sciences and Technology, Department of Civil Engineering, Tebessa, Algeria.

Submitted on July 27, 2020; Final Acceptance on February 10, 2021; Discussion open until May 31, 2021.

DOI: <https://doi.org/10.28927/SR.2021.055920>



This is an Open Access article distributed under the terms of the Creative Commons Attribution License, which permits unrestricted use, distribution, and reproduction in any medium, provided the original work is properly cited.

study based on the Plaxis software. The results obtained from this study confirmed that the stresses under the strip footing were augmented by 40% when the rock was encountered under the middle of the footing at a depth D of 0.5 m. Additionally, the stresses under the footing were altered when the buried rock was positioned away from the middle footing to the instability of the footing. Hussein (2014) presented results of finite element analysis for the stability of strip footing over circular continuous voids on sand. An equation was derived to define the relationship between the bearing capacity ratio and influencing feature. This equation provides a database for the design of continuous footing with an underground void at its centre. Lee et al. (2014) presented design charts estimating the undrained bearing capacity aspects as part of dimensionless factors connected to the vertical and horizontal cavity space from the footing, cavity size, and spacing between the two cavities, which contribute to soil rigidity and inconsistency. The ultimate bearing capacity is controlled by three different failures modes.

To explore the effect of inclination load on the bearing capacity of shallow continuous foundations situated on undrained clay soil with single and dual continuous cavities, small strain finite element analyses were performed by Lee et al. (2015). Additionally, they studied the influence of the position, form, and number of continuous voids. The results obtained are illustrated as normalized failure envelopes in the horizontal and vertical loading planes. Lavasan et al. (2016) numerically examined the bearing capacity and failure mechanism of a shallow strip foundation built above twin voids. The results obtained can be used to sketch the pattern of a footing on a cavity while the obtained failure mechanisms can be selected to improve analytical solutions. Moreover, it was inferred that a significant depth of the cavities and a critical space between them appear where the ultimate bearing capacity of the footing disappears. To study the impact of voids on the behaviour of strip footing under oblique load, Al-Jazaairry & Toma-Sabbagh (2017) applied the finite element analysis. They studied several footing cases, and in each case, an important depth appeared under which the existence of voids exposed the footing presented to minimum damage. When cavities were set up on this depth, the bearing capacity of the foundation varied according to the influence of many factors (position, size of the cavity, footing depth). The results obtained can be applied to create a shallow foundation laid on cavitied soil while the attained failure mechanisms can be utilized to develop numerical explanations to this sort of challenges. Zhou et al. (2018) examined the bearing capacity and failure mechanism of a perpendicular laden strip foundation on cohesive soil with square voids. The results indicate that the undrained bearing capacity with voids reacts to soil characteristics. The failure mechanism is linked to multiple soil properties, position of single voids, and straight space between two voids. Zhao et al. (2018) via the upper bound method carried out a study on the stability analysis of asymmetrical cavities. The results show that the stability numbers are augmented with an increase in the friction angle, but reduce with an increase in the horizontal

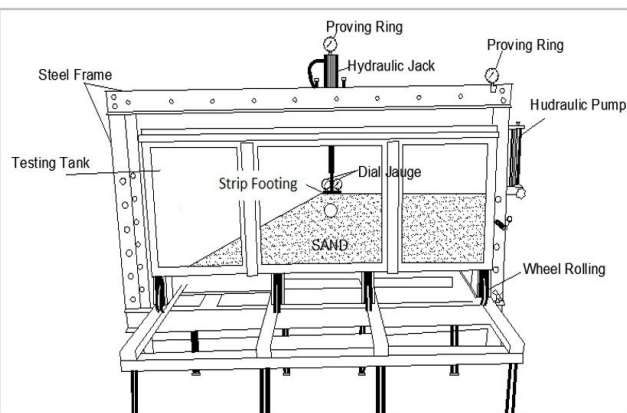
distance and descriptor diameter values, with considerable asymmetrical failure mechanisms. The results also indicate that the major failure type for the soil near the cavity is the local shear failure. A clear bottom bulge fact is detected in the void at its small inner. Based on their results, Piro et al. (2018) noticed that a novel equivalent wave parameter was accurately defined to take into consideration the existence of the underground level and cavities in seismic soil-foundation-structure interactions. Then they suggested relationships between the most significant parameters controlling the interaction phenomena. Xiao et al. (2018a) examined the effects of voids on the bearing capacity of strip footing under the plane-strain state, where a reduction factor was delineated. The obtained results are illustrated in different design charts, and the critical failure mechanisms are represented. Xiao et al. (2018b) used finite element limit analysis to study the undrained bearing capacity of strip footing on voids in two-layered clays. Design charts and equations are presented to estimate the undrained bearing capacity factor N_s . The effect of the parameters on N_s has also been inspected, including the undrained shear stress ratio of the soil, thickness of the top layer, location, size, width, height, and spacing of the voids. Zhang et al. (2019) investigated the collapsed roof of deep circular voids in jointed rock masses via numerical analysis. The results are sketched in dimensionless stability diagrams and are compared with transformational findings conducted using the algorithm of an analytical upper bound solution. Then, based on the frictional Mohr-Coulomb model, and in accordance with the non-associated flow rule, Lee & Kim (2019) researched on the collapse of strip rigid foundations positioned on sandy soil with both single and dual continuous voids. The obtained results agree positively with existing theoretical and numerical solutions.

Throughout a series of laboratory-scale load tests, Jayamohan et al. (2019) investigated the impact of a subsoil cavity on the load-settlement behaviour of a strip foundation. The results show that the effect of cavities is significant when they reach a critical depth and eccentricity, after which the reinforced foundation bed develops the load-settlement behaviour of a soil with voids. Additionally, the existing subsoil cavities can lead to stress concentrations that trigger failure. Saadi et al. (2020) led an experimental inquiry on the impact of interference on the bearing capacity of dual adjoining foundations on a granular cavitied soil. The results revealed the influence of cavities and the interference of dual footings on the bearing capacity factor, as well as the efficiency factor. Then, the effects of the cavities vanished when the distance footings/cavities were greater than three.

The overall purpose of this study is to probe the impact of underground circular voids on the bearing-capacity behaviour of a shallow continuous footing located on the edge of a cohesionless slope ($b/B=0$) such as b is distance between foundation and the edge of a slope. To realise this objective, a strip pattern footing was experimented. Furthermore, a practical range of parameters were studied, such as the vertical distance of the top of void from the bottom of footing (H/B),



Figure 1. Experimental apparatus.



horizontal distance between cavities-footing centre (L/B), and various vertical load eccentricities (e/B).

2. Experimental apparatus

The experimental pattern tests were carried out in a tank with a dimension of $1.60 \times 0.60 \times 0.60$ m. Figure 1 presents an illustration of the tank, which is made from steel with an entirely transparent plexiglass plate as the front part, and propped up with eight wheels rolling on straight steel support girders. The purpose of the rollers is to pull the box from under the loading mechanism in order to empty it and re-fill the soil into it.

These girders were strongly setup on horizontal steel pillars. The Plexiglass allowed the observation of the slope. It ensured the visibility of the sample throughout preparation. It also allowed the observation of sand particles' deformation throughout the testing. However, because the impact of sand pressure and the applied load could compromise the strength of the Plexiglass, it was strengthened with two steel columns. The tank box was solid enough to support the plane strain conditions by reducing the out of plane displacement. To guarantee its solidity and prevent deformation, a thick steel plate was used to manufacture the tank. The interior parts of the tank are coated and well-polished to reduce friction with the sand as much as possible. Based on the research conducted by Ueno et al. (1998), the boundary effects were taken into account, as shown in Figure 2.

3. Footing

To implement the designed strip footing pattern, a thick steel plate consisting of a range of holes was utilized. Several holes were created on both sides (left and right) at a 10-mm distance from the centre hole of the footing to be used as foundation loading points, with the dimensions of 598 mm long, 100 mm wide (B), and 20 mm thick. Both ends of the testing footing were optimally lustrated and lubricated to diminish frictional contact with the rigid box borders. Then, to ensure rugosity, a layer of sand paper was fixed to the footing base. To maintain plane strain conditions, the footing length and tank width were approximately the same

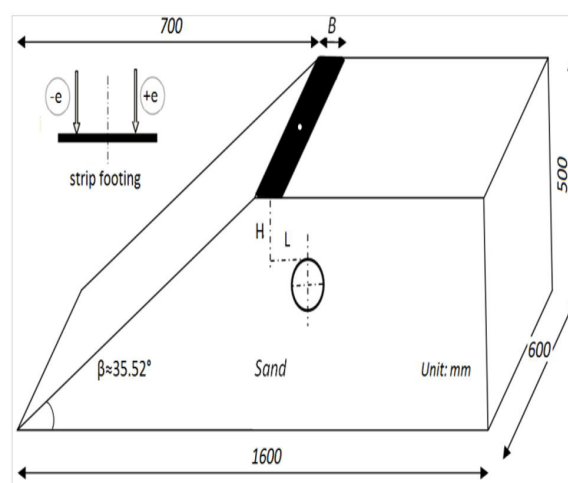


Figure 2. Geometry of the problem.

values. Then, ball bearing was employed to allow an easy loading to the footing.

4. Soil properties

This research is based on an intermediate to coarse sand that was cleaned, dried and filtered according to sand particles size'. It was collected from the south-east region of Algeria. Particles' size distribution was established following dry sieving technique and the findings are presented in Figure 3. A particular gravity of 2.65 was determined by picnometer test. The maximum and the minimum dry densities of the sand were measured and the corresponding values of the minimum and the maximum void ratio were calculated. To assess the friction angle, a series of direct shear tests at a relative sand density of 60% were performed. The residual friction angle of the compacted sand was about 37° , which matches to densified sand. Additional parameters of the tested sand are illustrated in Table 1.

5. Cavity properties

The purpose of using PVC in this work is to ensure the presence of cavity void, the thickness of PVC used is

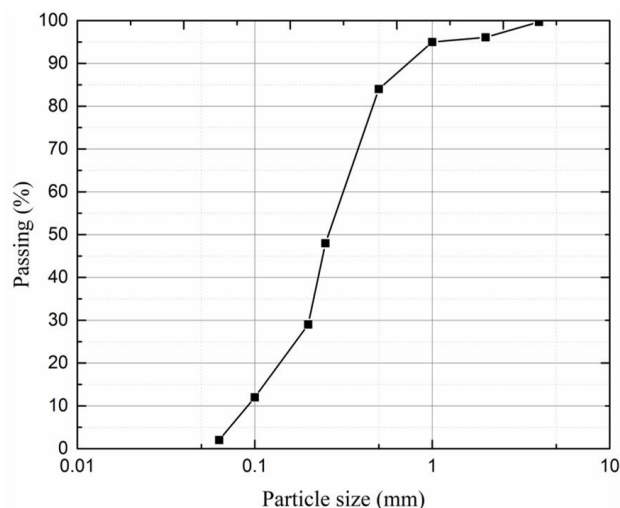


Figure 3. Grain size distribution curve of sand.

02 mm, the exterior diameter is 110 mm and the length is 558 mm. In the design of the test model, the parameters of the PVC tube are shown in Table 2.

6. Testing process

A total of 140 load bearing experimental tests were conducted on the strip footing pattern situated in close proximity to the crest slope. To improve the validity of the experiment, every single test was carried out thrice using parameters such as vertical distance between the void and footing (H/B), load eccentricity (e/B), and the horizontal distance void-footing centre (L/B). Then, based on the process presented by El Sawwaf (2004), the experimental slope sand angle was equal to 35.52° . After that, via a manual rammer, the used sand was densified in each layer- 50 mm thick up to 500 mm height, at a relative density according to the designed testing program, the desired relative density was achieved after carrying out several preliminary experiments using different compacted energies and layers thick. During the compaction process, a void was positioned in our soil sample via a circular PVC with a diameter of 100 mm and length of 598 mm. The PVC was set down in the required position and sand compaction continued until the final bed was achieved. Tests were carried out for diverse locations of voids and varied parameters, as presented in Table 3. The sand sample was formed in line with the slope shape and framed on the plexiglass side. The formed surfaces were first levelled, then the model footing was positioned on sand, with a predetermined alignment, such that the load could be vertically transferred to the footing. To preserve typical conditions throughout the testing programme, the tank was poured out and refilled for each test.

7. Results and discussion

A total of 140 tests were conducted on the bearing capacity of stiff continuous footing situated on the slope of a soil with various void positions, a range of eccentric

Table 1. Material properties of the sand used.

Property	Value
Specific gravity G_s	2.65
Uniformity coefficient C_u	3.19
Coefficient of curvature C_c	1.40
Maximum dry unit weight $\gamma_d(\max)$, kN/m^3	17.12
Minimum dry unit weight $\gamma_d(\min)$, kN/m^3	14.62
Peak friction angle ϕ^0	37

Table 2. Properties of the PVC used.

Parameters	Value
Density (kN/m^3)	13.5-14.6
Tensile strength (MPa)	45
Elongation %	80
Elastic modulus (MPa)	3000

Table 3. Model tests program.

Strip footing (mm)	H/B	L/B	Eccentricities e (mm)
100x598	0.5	0,1,2,3	-30, -20, -10, 0, 10, 20, 30
	1	0,1,2,3	-30, -20, -10, 0, 10, 20, 30
	1.5	0,1,2,3	-30, -20, -10, 0, 10, 20, 30
	2	0,1,2,3	-30, -20, -10, 0, 10, 20, 30
	3	0,1,2,3	-30, -20, -10, 0, 10, 20, 30

vertical loading ratios ($e/B = 0, \pm 0.1, \pm 0.2$, and ± 0.3), and constant footing space from slope crest ($b/B = 0$). The void positions moved horizontally (L/B) from the footing centre with alternating values between 0 and $3B$, and also vertically from the soil surface (H/B) with alternating values between $0.5B$ and $3B$, as presented in Table 1. A no-void reference test was also carried out.

To assess the validity and reliability of the small-scale laboratory test results, the bearing capacity was achieved by dividing the limit load on the area of footing. Ueno et al. (1998) tangent intersection method was used to set the bearing capacity results.

7.1 Effect of eccentricity

The influence of eccentric loading on bearing capacity is illustrated by the load-eccentricity curves (Figure 4) for different void locations and normalized slope/footing distances ($b/B = 0$).

It was established through the experimental results that the bearing capacity was considerably influenced by void presence and load eccentricities, here, the load diminished with an increase in the eccentricity ratio ($\pm e/B$). A significant increase in the bearing capacity value appeared when $e/B = +0.1$. Although this peculiarity can be explained in terms of load divergence from the crest's slope and the void centreline, at $e/B = +0.2$ and $e/B = +0.3$, a reversal of the footing was

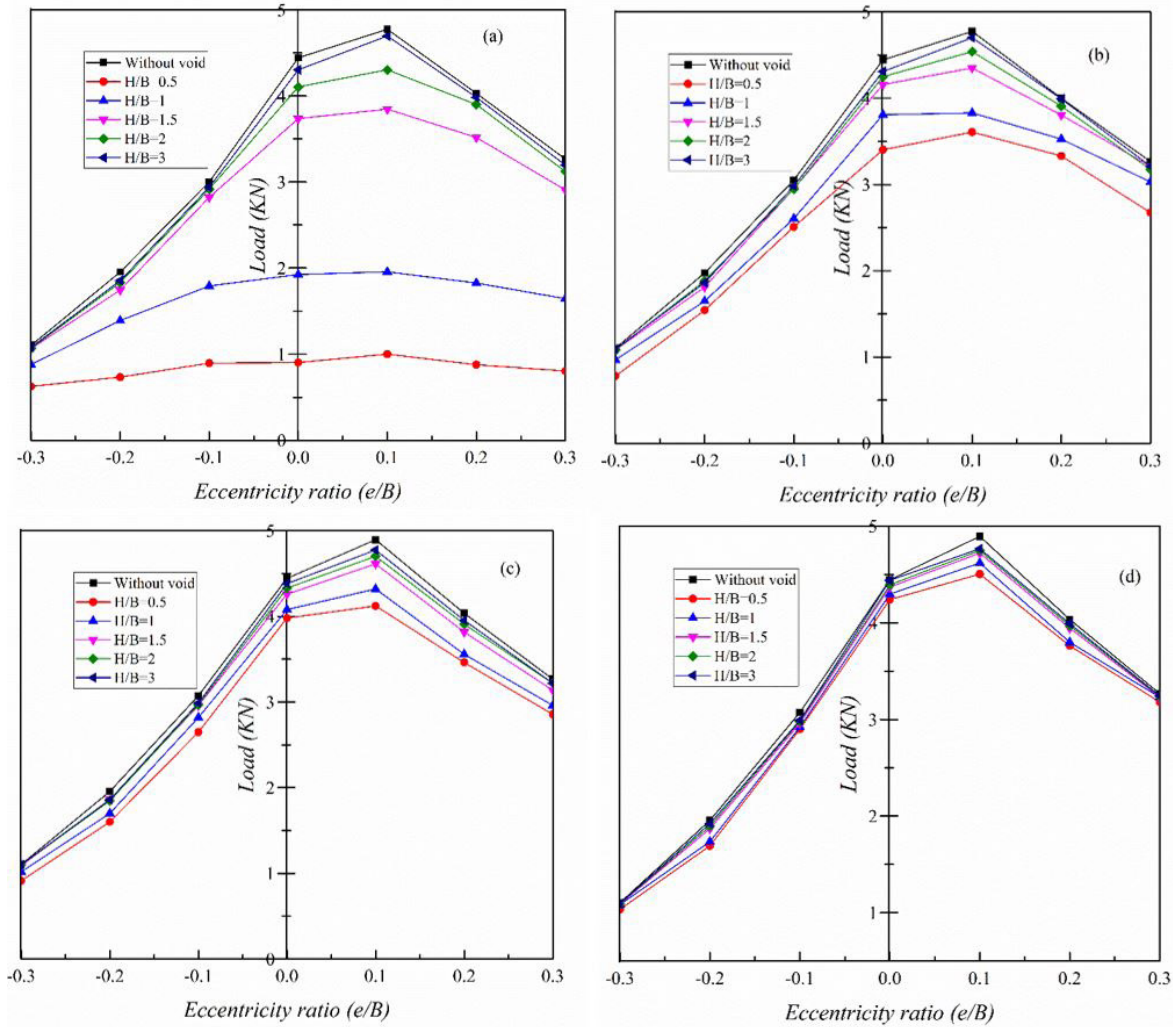


Figure 4. Load with variable eccentricities for void horizontal distance. (a) L/B=0; (b) L/B=1; (c) L/B=2; and (d) L/B=3.

observed, which occurred and gradually reduced the bearing capacity value.

Furthermore, the ultimate bearing capacity for a negative eccentric load is inferior to a positive one.

This signifies that the failure region under a positive eccentric loading is greater than that under a negative one. The gradual displacements shifted to the slope leaning, and a non-symmetrical failure mechanism was observed.

In contrast with the footing location, the passive region was imperfect, thus triggering a diminution in the bearing capacity.

7.2 The Effect of void’s depth

Figure 5 shows the effect of embedment depth, from the foundation base to the void’s crown, on the bearing pressure ratio of a strip foundation positioned on the edge of a sandy soil at different load eccentricities.

The obtained results were analysed in terms of a dimensionless parameter called bearing capacity ratio: i_H

$= q_v/q_{mv}$ where q_v represents the bearing capacity of the strip footing on the ground with a void while q_{mv} defines the ultimate bearing capacity for the same footing placed on the sand without void.

A significant instability between the soil and the nearby voids had been observed when the void distance H/B and L/B were equal to 0.5 and 0, respectively. Consequently, the soil collapsed with an 80% reduction in the bearing capacity value. This occurred because the small distance between the footing and void, including the soil mass underneath the footing was thin. Therefore, a low total shearing resistance was mobilized.

Then, an increase in the negative load eccentricity (direction of the slope) reduced the void embedding effect as we suspected. Moreover, the H/B effect was less influential for negative eccentricity than for positive eccentricity, this can be explained, that for negative eccentricity, the loading point moves away from the centre of the void and thus leads

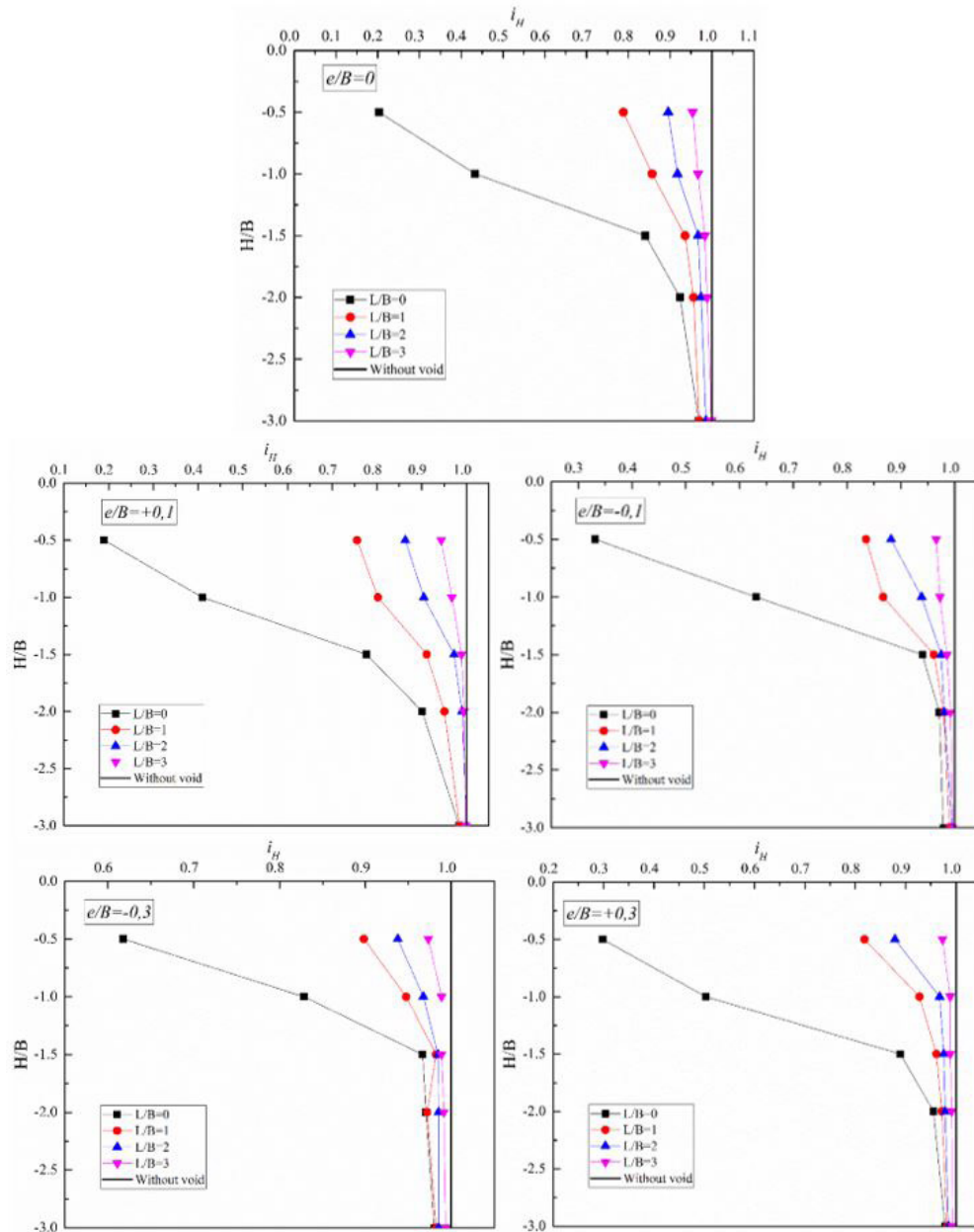


Figure 5. Effect of depth void with bearing capacity ratio.

to an increase in bearing capacity. Furthermore, in the cases at $H/B=1$ and $H/B=1.5$, notably, we observed the same impact for negative and positive load eccentricities but with less significant intensities.

As illustrated in Figure 5, irrespective of the eccentricity of the load and distance of the void from the centreline of the foundation, the bearing capacity ratio of the footing increases as the depth of the void's crown augments from a footing bottom, which reaches a maximum value at $H/B = 2$. This specific depth is called 'critical depth' and it was also determined by (Badié & Wang, 1984). Beyond this depth, the influence of the void on the bearing pressure ratio

appeared to be the same as that of a footing without a void. Additionally, the values converged to the reference case. This behaviour occurs owing to the voids distant from the shear zone. Therefore, the failure mechanism formed was similar to that of the no-void. Finally, it was determined that when $L/B = 3$, the H/B effect is negligible.

7.3 The effect of void horizontal distance from foundation centreline

To probe the effect of the horizontal distance, several curves were plotted, as shown in Figures 6a, b, c, d. The results show that at $L/B=2$ and $L/B=3$, the effect of the void on the bearing capacity of a foundation under eccentric loads

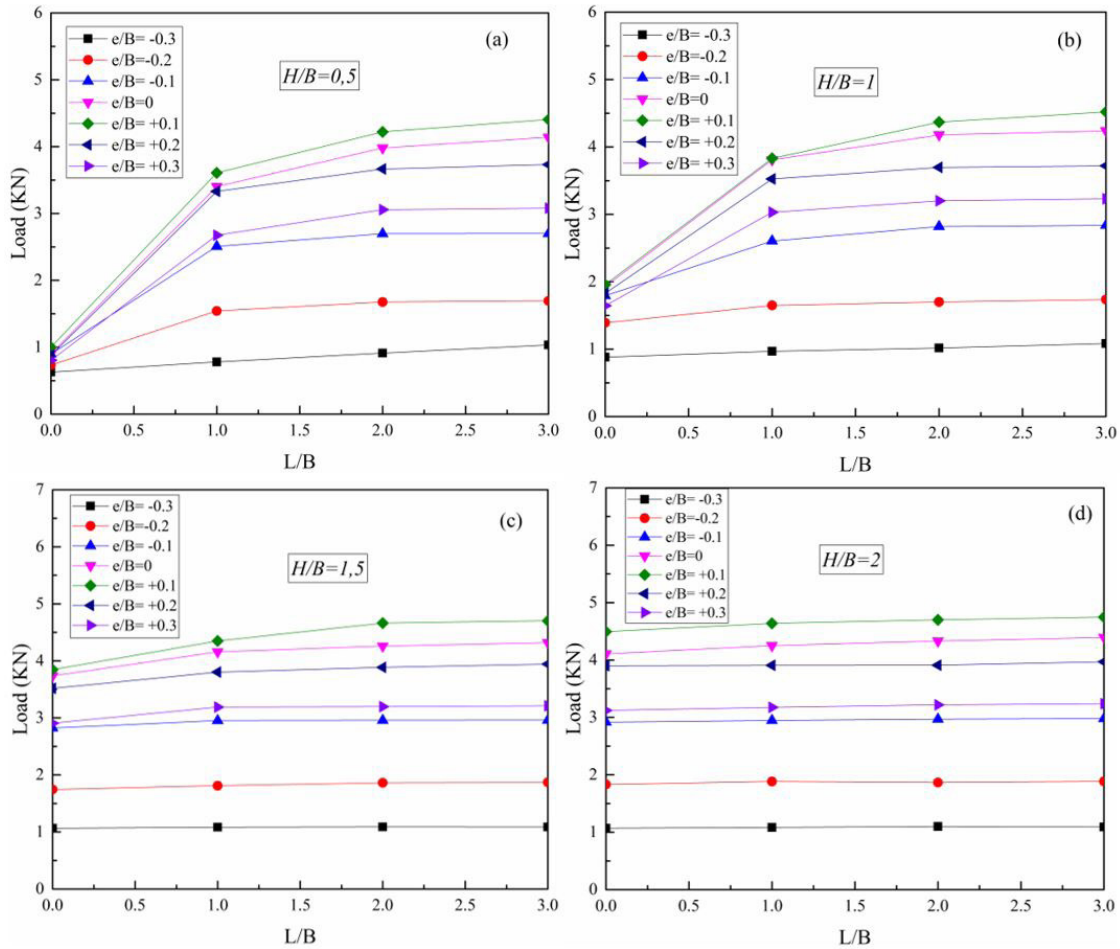


Figure 6. Effect of load with horizontal distance from foundation centreline. a) $H/B=0.5$; b) $H/B=1$; c) $H/B=1.5$ and d) $H/B=2$.

is annulled, and the behaviour of the footing is similar to that of a no-void foundation.

In Figure 6, it was set up such that for $H/B = 0.5$ and $H/B = 1$, the influence of the eccentricities on the bearing capacity was nearly negligible as the void moved closer to the base of the footing. For the other void depths, it can be observed that the curves converge towards the case without a void.

According to the test results presented in Figure 6, curves were designed at various void horizontal distances shifting from 0 to 3 B. Irrespective of the eccentricity of the applied load ($e/B = -0.3, -0.2, -0.1, 0.0, +0.1, +0.2, +0.3$), the void moves far away from the centreline footing, thus indicating a decrease in its influence. Moreover, its impact becomes insignificant when the void divergence equals twice the width of the footing. Beyond $H/B = 2$, the foundation behaves like a foundation without a void, as shown in Figure 6d.

A careful examination reveals that in the case of $e/B = -0.3$ and $e/B = -0.2$, the effect of the slope controls the behaviour of the foundation, whereas the effect of the horizontal distance is insignificant. Furthermore, owing to load eccentricity, the footing started to lose contact with the soil.

8. Conclusion

In this study, various performed laboratory tests were conducted to determine the impact of underground circular voids on the bearing-capacity behaviour of a shallow continuous footing located on the edge of a cohesionless slope ($b/B=0$). Based on the obtained results, the following findings and conclusions were made:

- The results prove that the bearing capacity is considerably influenced by the location of the void and load eccentricity;
- The ultimate bearing capacity for a positive eccentric load is greater than that of a negative one owing to the slope presence and underlying void;
- Because the soil mass underneath the footing is thin, the short distance between the footing and void leads to soil collapse along with a significant decrease in bearing capacity, thus mobilizing a low total shearing resistance is mobilized;
- The negative load eccentricity (direction of the slope) reduces the effect of void inclusion, whereas the effect of H/B is less significant on the negative eccentricity than on positive eccentricity;

- Irrespective of the eccentricity of the load and distance of the void from the centreline of the foundation, the bearing capacity of the footing increases as the depth of the void's crown augments till it reaches a maximum value at $H/B = 2$. Beyond this depth, the influence of the void on the bearing pressure appears to be the same as that of a footing without a void;
- In the case where the horizontal distance of the void from the foundation centreline equals three times the footing width, the effect of the void's depth is negligible;
- The impact of eccentricities on the bearing capacity is nearly negligible when the void moves closer to the base of the footing;
- The influence of the void is insignificant when the void is placed at a depth equivalent to 2 times the width of the footing;
- Regardless of the eccentricity of the applied load, the influence of the void gradually reduces as the void moves far away from the footing centreline, and its impact becomes more negligible when void divergence equals twice the width of the footing.

Declaration of interest

We have no conflicts of interest to disclose.

Author's contributions

Tarek Mansouri: methodology, investigation, data curation, writing - original draft preparation. Rafik Boufarh: conceptualization, supervision, validation. Djamel Saadi: data curation, writing - reviewing and editing.

References

- Al-Jazairry, A.A., & Toma-Sabbagh, T.M. (2017). Effect of cavities on the behaviour of strip footing subjected to inclined load. *International Journal of Civil, Environmental, Structural, Construction and Architectural Engineering*, 11(3), 292-298.
- Atkinson, J.H., & Potts, D.M. (1977). Stability of a shallow circular tunnel in cohesionless soil. *Geotechnique*, 27(2), 203-215. <http://dx.doi.org/10.1680/geot.1977.27.2.203>.
- Badie, A., & Wang, M.C. (1984). Stability of spread footing above void in clay. *Journal of Geotechnical Engineering*, 110(11), 1591-1605. [http://dx.doi.org/10.1061/\(ASCE\)0733-9410\(1984\)110:11\(1591\)](http://dx.doi.org/10.1061/(ASCE)0733-9410(1984)110:11(1591)).
- Baus, R.L., & Wang, M.C. (1983). Bearing capacity of strip footing above void. *Journal of Geotechnical Engineering*, 109(1), 1-14. [http://dx.doi.org/10.1061/\(ASCE\)0733-9410\(1983\)109:1\(1\)](http://dx.doi.org/10.1061/(ASCE)0733-9410(1983)109:1(1)).
- Culshaw, M.G., & Waltham, A.C. (1987). Natural and artificial cavities as ground engineering hazards. *Quarterly Journal of Engineering Geology*, 20(2), 139-150. <http://dx.doi.org/10.1144/GSL.QJEG.1987.020.02.04>.
- El Sawwaf, M.A. (2004). Strip footing behavior on pile and sheet pile-stabilized sand slope. *Alexandria Engineering Journal*, 43(1), 41-54. [http://dx.doi.org/10.1061/\(asce\)1090-0241\(2005\)131:6\(705\)](http://dx.doi.org/10.1061/(asce)1090-0241(2005)131:6(705)).
- Hussein, M.M.A. (2014). Stability of strip footing on sand bed with circular void. *Journal of Engineering Sciences*, 42(1), 1-17. <http://dx.doi.org/10.21608/jesaun.2014.111011>.
- Jayamohan, J., Shajahan, T., & Sasikumar, A. (2019). Effect of underground void on the internal stress distribution in soil. In T. Thyagaraj (Ed.), *Ground improvement techniques and geosynthetics* (Lecture Notes in Civil Engineering, No. 14, pp. 45-56). Singapore: Springer. https://doi.org/10.1007/978-981-13-0559-7_6.
- Khalil, A.A., & Khattab, S.A. (2009). Effect of cavity on Stress distribution and Settlement under Foundation. *AL-Rafdain Engineering Journal*, 17(6), 14-29. <http://dx.doi.org/10.33899/rengj.2009.43621>.
- Kiyosumi, M., Kusakabe, O., & Ohuchi, M. (2011). Model Tests and analyses of bearing capacity of strip footing on stiff ground with voids. *Journal of Geotechnical and Geoenvironmental Engineering*, 137(4), 363-375. [http://dx.doi.org/10.1061/\(ASCE\)GT.1943-5606.0000440](http://dx.doi.org/10.1061/(ASCE)GT.1943-5606.0000440).
- Kiyosumi, M., Kusakabe, O., Ohuchi, M., & Le Peng, F. (2007). Yielding pressure of spread footing above multiple voids. *Journal of Geotechnical and Geoenvironmental Engineering*, 133(12), 1522-1531. [http://dx.doi.org/10.1061/\(ASCE\)1090-0241\(2007\)133:12\(1522\)](http://dx.doi.org/10.1061/(ASCE)1090-0241(2007)133:12(1522)).
- Lavasan, A.A., Talsaz, A., Ghazavi, M., & Schanz, T. (2016). Behavior of shallow strip footing on twin voids. *Geotechnical and Geological Engineering*, 34(6), 1791-1805. <http://dx.doi.org/10.1007/s10706-016-9989-6>.
- Lee, J.K., & Kim, J. (2019). Stability charts for sustainable infrastructure: collapse loads of footings on sandy soil with voids. *Sustainability*, 11(14), 3966. <http://dx.doi.org/10.3390/su11143966>.
- Lee, J.K., Jeong, S., & Ko, J. (2014). Undrained stability of surface strip footings above voids. *Computers and Geotechnics*, 62, 128-135. <http://dx.doi.org/10.1016/j.compgeo.2014.07.009>.
- Lee, J.K., Jeong, S., & Ko, J. (2015). Effect of load inclination on the undrained bearing capacity of surface spread footings above voids. *Computers and Geotechnics*, 66, 245-252. <http://dx.doi.org/10.1016/j.compgeo.2015.02.003>.
- Mohamed, A.K. (2012). Numerical study for the behavior of strip footing on sand in the existence of a buried rock. *JES. Journal of Engineering Sciences*, 40(6), 1611-1624. <http://dx.doi.org/10.21608/jesaun.2012.114532>.
- Piro, A., Silva, F., Di Santolo, A.S., Parisi, F., & Silvestri, F. (2018). Sensitivity analysis of seismic soil-foundation-structure interaction in masonry buildings founded on cavities. In *Proceedings of the 16th European Conference on Earthquake Engineering* (pp. 1-10), Thessaloniki.
- Saadi, D., Abbeche, K., & Boufarh, R. (2020). Model experiments to assess effect of cavities on bearing capacity of two interfering superficial foundations resting on granular soil. *Studia Geotechnica et Mechanica*, 42(3), 222-231. <http://dx.doi.org/10.2478/sgem-2019-0046>.

- Ueno, K., Miura, K., & Maeda, Y. (1998). Prediction of ultimate bearing capacity of surface footings with regard to size effects. *Soil and Foundation*, 38(3), 165-178. http://dx.doi.org/10.3208/sandf.38.3_165.
- Wang, M.C., & Badie, A. (1985). Effect of underground void on foundation stability. *Journal of Geotechnical Engineering*, 111(8), 1008-1019. [http://dx.doi.org/10.1061/\(ASCE\)0733-9410\(1985\)111:8\(1008\)](http://dx.doi.org/10.1061/(ASCE)0733-9410(1985)111:8(1008)).
- Wang, M.C., & Hsieh, C.W. (1987). Collapse load of strip footing above circular void. *Journal of Geotechnical Engineering*, 113(5), 511-515. [http://dx.doi.org/10.1061/\(ASCE\)0733-9410\(1987\)113:5\(511\)](http://dx.doi.org/10.1061/(ASCE)0733-9410(1987)113:5(511)).
- Xiao, Y., Zhao, M., & Zhao, H. (2018a). Undrained stability of strip footing above voids in two-layered clays by finite element limit analysis. *Computers and Geotechnics*, 97, 124-133. <http://dx.doi.org/10.1016/j.compgeo.2018.01.005>.
- Xiao, Y., Zhao, M., Zhao, H., & Zhang, R. (2018b). Finite Element Limit Analysis of the Bearing Capacity of Strip Footing on a Rock Mass with Voids. *International Journal of Geomechanics*, 18(9), 04018108. [http://dx.doi.org/10.1061/\(ASCE\)GM.1943-5622.0001262](http://dx.doi.org/10.1061/(ASCE)GM.1943-5622.0001262).
- Zhang, R., Chen, G., Zou, J., Zhao, L., & Jiang, C. (2019). Study on roof collapse of deep circular cavities in jointed rock masses using adaptive finite element limit analysis. *Computers and Geotechnics*, 111, 42-55. <http://dx.doi.org/10.1016/j.compgeo.2019.03.003>.
- Zhao, L., Huang, S., Zhang, R., & Zuo, S. (2018). Stability analysis of irregular cavities using upper bound finite element limit analysis method. *Computers and Geotechnics*, 103, 1-12. <http://dx.doi.org/10.1016/j.compgeo.2018.06.018>.
- Zhou, H., Zheng, G., He, X., Xu, X., Zhang, T., & Yang, X. (2018). Bearing capacity of strip footings on $c-\phi$ soils with square voids. *Acta Geotechnica*, 13(3), 747-755. <http://dx.doi.org/10.1007/s11440-018-0630-0>.

List of symbols

(B): width of footing

(b): distance between foundation and the edge of a slope

($\pm e$): positive, negative eccentric load

(H): top vertical distance of the void from the base of footing.

(L): horizontal distance between cavities-footing centre (L/B).

Ns: undrained bearing capacity factor.

(Gs): Specific gravity

(Cu): Uniformity coefficient

(Cc): Coefficient of curvature

($\gamma_d(\max)$): maximum dry unit weight

($\gamma_d(\min)$): minimum dry unit weight

(ϕ): Peak friction angle

(β): slope angle

PVC: (abbreviation coming from the English name (polyvinyl chloride)

(iH): dimensionless parameter called bearing capacity ratio

(qv): ultimate bearing capacity of the strip footing placed on the sand with a void

(qnv): ultimate bearing capacity of the strip footing placed on the sand without void.